

Spin-orbit selectivity observed for the $\text{HCl}^+(\tilde{X}^2\Pi)$ state using resonant photoemission

R. F. Fink,* F. Burmeister, R. Feifel, M. Bässler, O. Björneholm, L. Karlsson, C. Miron, and M.-N. Piancastelli
Department of Physics, Uppsala University, Box 530, S-751 21 Uppsala, Sweden

S. L. Sorensen

Department of Synchrotron Radiation Research, Institute of Physics, University of Lund, Box 118, S-221 00 Lund, Sweden

H. Wang, K. Wiesner, and S. Svensson†

Department of Physics, Uppsala University, Box 530, S-751 21 Uppsala, Sweden

(Received 2 February 2001; published 13 February 2002)

We report the experimental observation of a strongly selective population of the spin-orbit components in the $\text{HCl}^+ \tilde{X}^2\Pi_\Omega$ states after excitation into the dissociative $2p^{-1}6\sigma^*$ core excited state. A progression of highly excited vibrational states with either the $\Omega=3/2$ or $\Omega=1/2$ component of the final state is populated, respectively, when the excitation is tuned in the $2p_{3/2}^{-1}6\sigma^*$ or $2p_{1/2}^{-1}6\sigma^*$ part of the resonance. This effect is explained theoretically to be due to the orientational selectivity of the excitation process and the preference of the $L_{2,3}VV$ Auger process to produce valence holes with the same orientation as the core holes.

DOI: 10.1103/PhysRevA.65.034705

PACS number(s): 33.80.Eh, 33.70.Ca, 34.50.Gb

Photoemission spectroscopy is one of the most frequently used methods for the investigation of the electronic structure of matter. Using a one-particle picture, the excitation of electrons from all occupied orbitals is allowed with comparable probability. However, a discrimination of the ionization from certain orbitals is generally not possible with this method. The latter is particularly true if the constitution of the orbitals is similar as, e.g., in the case of degenerate orbitals that are split by spin-orbit interaction. In general, this property of the photoionization process is an advantage as it allows to obtain a rather complete picture of the electronic structure. If such a method of discrimination existed and if its mechanism was well understood, it would be useful for getting more insight from the results of this technique. One possibility to change the selectivity of photoemission spectroscopy is by tuning the excitation energy through an autoionizing resonance, as this changes the intensity distributions between electronic and, for molecules, also vibrational final states [1–3].

In this paper we investigate resonant photoemission of HCl through an autoionizing resonance to the spin-orbit split $\tilde{X}^2\Pi_{1/2}$ and $\tilde{X}^2\Pi_{3/2}$ final states of HCl^+ . While direct photoemission [4] and resonant photoemission via an autoionizing valence state [5] lead to both spin-orbit components with about the same probability, we find that resonant photoemission via the dissociative $\text{Cl } 2p^{-1}6\sigma^*$ core-excited state causes a pronounced (>90%) selectivity of either one or the other spin-orbit component depending on whether the excitation is tuned to the $2p_{3/2}^{-1}6\sigma^*$ or $2p_{1/2}^{-1}6\sigma^*$ component of the resonance. We investigate the origin of this selectivity and discuss the implications of this phenomenon.

The spectra were recorded at beam line I411 [6] at the MAX II storage ring in Lund, Sweden. The beam line is

equipped with a modified Zeiss SX-700 plane-grating monochromator and with a rotatable hemispherical Scienta SES-200 high-resolution electron spectrometer. The exciting photon bandwidth (full width at half maximum) was set to 45 meV and the spectrometer resolution was 40 meV for all spectra, thus giving a total resolution of 60 meV. The main axis of the spectrometer lens was set at the magic angle (54.7°) with respect to the polarization vector of the undulator radiation. HCl gas was obtained commercially from Air Liquide with a stated purity of >99.99% and DCl gas of comparable purity was produced by us. The purity of both gases has been carefully checked by on-line valence photoelectron spectroscopy during measurements. The photon energy was determined by electron yield spectra around the $\text{HCl } 2p^{-1}6\sigma^*$ resonance recorded before and after all resonant photoemission spectra. The binding energy was calibrated relative to valence-band spectra from Ref. [7].

HCl and DCl molecules were exposed to synchrotron light tuned to the dissociative $2p_{3/2}^{-1}6\sigma^*$ and $2p_{1/2}^{-1}6\sigma^*$ resonances at 200.6 eV and 202.7 eV, respectively, and to 190 eV (off resonance). The corresponding electron spectra are shown in Fig. 1 on a binding-energy scale. For all excitation energies the dominant process is direct photoemission of the 2π orbital leading to the spin-orbit split $^2\Pi_{3/2}$ and $^2\Pi_{1/2}$ states of HCl^+ . As the potential-energy curves of these states and the HCl ground state are almost parallel, the Franck-Condon principle causes that only vibrational levels $\nu''=0, 1, \text{ and } 2$ can be observed for the direct process. However, if the excitation energy is tuned in one of the $2p^{-1}6\sigma^*$ resonances (upper panel of Fig. 1), then a vibrational progression up to $\nu''=13$, about 16 eV binding energy, can be observed. At higher binding energies, the overlap with the $\tilde{A}^2\Sigma^+$ state with an adiabatic binding energy of 16.268 eV [7] sets in, making it impossible to follow the progression further. This extension of the vibrational progression is due to the mechanism indicated in Fig. 2. Photoabsorption leads preferentially to two $2p^{-1}6\sigma^*$ excited states, which dissociate and au-

*Also at Theoretical Chemistry, University of Lund, Box 124, S-221 00 Lund, Sweden.

†Corresponding author. Fax: +46-18 471 35 24. Email address: svante.svensson@fysik.uu.se

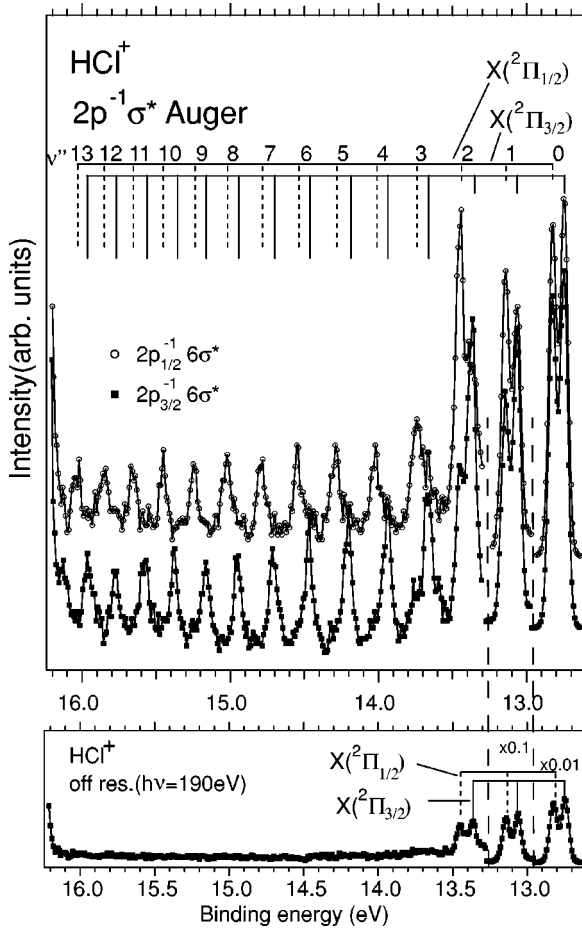


FIG. 1. Photoemission spectra of HCl showing the $\text{HCl}^+ \bar{X}^2\Pi$ final state.

to ionize on the same time scale. The connected probability of the vibrational wave function at extended bond distances leads to the pronounced changes in the vibrational progressions. In prior work this process has been investigated in much detail, in particular, with respect to consequences for the dissociation process and spectroscopical features [8–14].

In this paper we consider another striking feature of these spectra: whereas direct photoionization populates both spin-orbit components (see $\nu'' \leq 2$ final states in Fig. 1), the vibrational excitations above $\nu'' = 2$, which are only populated in the resonant process, are governed by a propensity rule favoring occupation of the $^2\Pi_{3/2}$ ($^2\Pi_{1/2}$) ionic states upon excitation of the $2p_{3/2}^{-1}6\sigma^*$ ($2p_{1/2}^{-1}6\sigma^*$) resonant neutral states. The resonant process appears to transfer the j quantum number of the intermediate-state $2p$ hole into the Ω quantum number of the ionic $^2\Pi_{\Omega}$ final state.

The spectra equivalent to Fig. 1 for DCl^+ (not presented in this paper) show a smaller vibrational spacing but the same spin-orbit selectivity. Thus, the underlying mechanism must lie in the electronic properties of resonant photoemission rather than in its nuclear dynamics.

In the following we give a theoretical explanation of the observed propensity, which is based on results of detailed *ab initio* calculations that were made for both the excitation and for the Auger decay processes with the methods described in

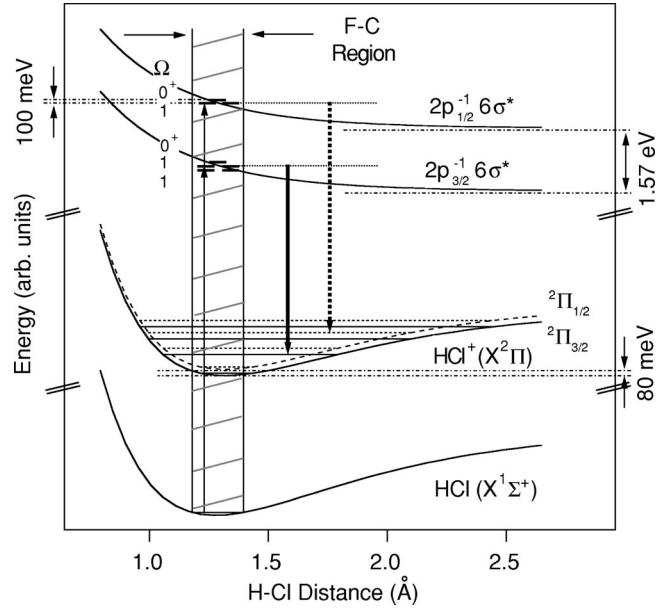


FIG. 2. Energy diagram explaining the transitions between the initial, intermediate, and final ionic states. The dashed (full) lines refer to the $^2\Pi_{1/2}$ ($^2\Pi_{3/2}$) final ionic state. The corresponding transitions are indicated similarly by dashed and full arrows.

Refs. [15,16]. The results shown here were obtained at the equilibrium bond distance of the HCl ground state but the same calculations were also performed at extended bond distances.

The key feature for understanding the observed effect is based upon the electronic structure of the $\text{Cl } 2p^{-1}6\sigma^*$ core-excited state, which can be related to the electronic structure of the $\text{Cl } 2p$ ionized HCl molecule [16–19]. The energies of the three $\text{Cl } 2p^{-1}$ levels are shown in the left part of Fig. 3. A spin-orbit splitting of about 1.6 eV separates the $2p_{1/2,m_j}$ and $2p_{3/2,m_j}$ levels. Note that only the m_j quantum number (which is usually called ω in this context) is a good quantum

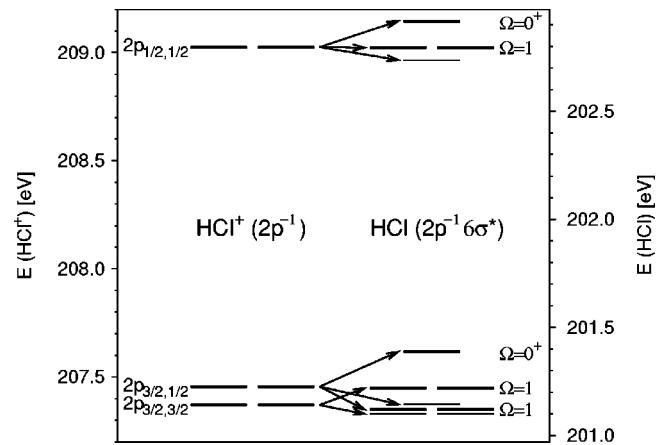


FIG. 3. Energy-level scheme of the $2p$ ionized HCl molecule (left side, naming according to the dominating core hole) and the correlation with the $(2p^{-1}6\sigma^*)$ core-excited states (right side). In the latter the dipole-allowed (-forbidden) $\Omega = 1$ and $\Omega = 0^+$ ($\Omega = 2$ and $\Omega = 0^-$) states are represented with thick (thin) lines.

TABLE I. Calculated properties of the $2p^{-1}6\sigma^*$ excited states: Vertical excitation energies E from the HCl ground state, their oscillator strengths f , the contribution of the jj -coupled ($2p_{j,m_j}^{-1}6\sigma^*$) configurations to the intermediate-state wave function, and Auger transition rates $\Gamma_f(^2\Pi_\Omega)$ in $\mu\text{a.u.}$ for the transitions to the $^2\Pi_\Omega$ final ionic states.

No.	Ω	E (eV)	$10^3 f$	Contribution to the wave function			$\Gamma_f(^2\Pi_{1/2})$	$\Gamma_f(^2\Pi_{3/2})$
				$2p_{1/2,1/2}^{-1}6\sigma^*$	$2p_{3/2,1/2}^{-1}6\sigma^*$	$2p_{3/2,3/2}^{-1}6\sigma^*$		
1	0^+	201.380	0.640	0.021	0.979		2552	2552
2	0^+	202.909	0.597	0.979	0.021		2813	2813
1	1	201.107	0.044	0.000	0.686	0.314	404	497
2	1	201.213	8.096	0.002	0.314	0.684	68	775
3	1	202.786	5.034	0.998	0.000	0.002	836	36

number of the HCl ion. A much smaller molecular field splitting of 0.085 eV [17] splits the otherwise fourfold degenerate $2p_{3/2}$ hole states into two Kramers doublets. This splitting arises because of the different spatial orientations of the $2p_{3/2,3/2}$ and $2p_{3/2,1/2}$ orbitals with respect to the bond axis of the molecule. It has been verified with accurate theoretical calculations [16,18], and its influence on experimental photoelectron [17,19] and Auger electron [16,19] spectra has been discussed.

If now one electron is put into the antibonding $6\sigma^*$ valence orbital of the core-ionized HCl molecule (right side of Fig. 3), the system is lowered by an average energy of 6.23 eV as is apparent from the different energy scales in the figure. The detailed structure is further influenced by exchange interactions of the $2p$ core holes and the $6\sigma^*$ electron, which are slightly larger than the molecular field splitting discussed above for the HCl^+ ($2p^{-1}$) states. The arrows in Fig. 3 indicate the major correlations between the core-ionized states of HCl^+ and those of the $2p^{-1}6\sigma^*$ -excited HCl molecule. The good quantum number Ω results from the coupling of the electron in the $6\sigma^*$ orbital with $\omega=1/2$ to the ω quantum number of the corresponding HCl^+ state. For the present case of strong spin-orbit coupling the double-group symmetry symbols $\Omega=0^\pm, 1$, and 2 are appropriate. They correspond to the Σ^\pm, Π , and Δ point-group symmetries, respectively (see, e.g., [20]).

The numerical amount of the Cl $2p_{j,m_j}$ hole configurations in the intermediate state wave function is listed in Table I. This corroborates the qualitative assignment indicated in Fig. 3, but the two $\Omega=1$ states related to the $2p_{3/2}^{-1}$ core hole are significantly coupled. The oscillator strengths in the table show that excitation to the Cl $2p_{3/2}^{-1}6\sigma^*$ and Cl $2p_{1/2}^{-1}6\sigma^*$ resonances leads almost exclusively to the second and third $\Omega=1$ states. Thus, for the following discussion we will restrict ourselves to the resonant decay of these two states, i.e., the two lowest rows of Table I.

The calculated Auger transition rates reproduce the observed selectivity in the population of the spin-orbit components. An analysis of the intermediate-state wave functions suggests a simple explanation: If the HCl molecule is excited in the $2p_{3/2}^{-1}6\sigma^*$ ($2p_{1/2}^{-1}6\sigma^*$) resonance, then the second (third) $\Omega=1$ state is populated; this state consists preferentially of the Cl $2p_{3/2,3/2}$ ($2p_{1/2,1/2}$) hole. Thus, the Auger process transfers the m_j or ω quantum number of the $2p$ core

hole of the intermediate state to the generated final-state 2π hole. However, whereas this gives a correct qualitative and quantitative explanation for the $2p_{1/2}^{-1}6\sigma^*$ resonance, it underestimates the 90% selectivity measured in the spectrum via the $2p_{3/2}^{-1}6\sigma^*$ resonance. In Table I we see that the corresponding second $\Omega=1$ state consists of 68% of the Cl $2p_{3/2,3/2}$ and 32% of the Cl $2p_{j,1/2}$ core-hole configurations. A more detailed analysis of the theoretical results shows the following.

(i) The calculated selectivity at the equilibrium bond distance of HCl is higher than 68% as the Cl $2p_{3/2,3/2}^{-1}6\sigma^*$ and Cl $2p_{3/2,1/2}^{-1}6\sigma^*$ configurations have both a non-negligible decay rate to both spin-orbit components. By a positive and negative interferencelike mechanism this causes the observed high selectivity.

(ii) At larger internuclear distances, where most of the observed Auger decay happens (Fig. 2), the wave function changes. Then the amount of the $2p_{3/2,3/2}^{-1}6\sigma^*$ configuration increases significantly, making the simple explanation from above quantitatively correct.

Can we expect the present propensity to be completely general? No. A look at Table I tells us that a necessary condition for this spin-orbit selectivity is that the intermediate-state wave function does not belong to the totally symmetric double-group representation. If the intermediate state is totally symmetric (as for the $\Omega=0^+$ states), then for symmetry reasons a completely equal population of the two spin-orbit components results. One should also notice that for the decay of the first $\Omega=1$ state both spin-orbit components are predicted to be populated with about equal probability.

A preference for some spin-orbit split configurations was observed in the normal $L_{2,3}M_{2,3}M_{2,3}$ Auger decay of the argon atom (see, e.g., [21] and references therein). However, in the atomic case selectivity is much less pronounced and has never been considered in much detail. One should stress that the reduced symmetry of the molecule produces this much more pronounced electronic selectivity. The current findings are related to prior observations for the $L_{2,3}VV$ Auger decay of H_2S [22,23]. Here the $\bar{X}^1A_1(2b_1^{-2})$ final state is populated only if the $S2p^{-1}$ core-ionized state has a significant contribution of the $1b_1$ core orbital, indicating, as in the

present case, strong coupling of the $2p$ core hole to the final-state valence hole.

In conclusion, we have observed a new propensity mechanism that makes it possible to select the spin-orbit component of the final state in the resonant Auger transition of a molecule. The theoretical explanation involves the explicit forms of the wave functions and it is predicted that similar cases can be seen for other nonsymmetric intermediate states.

We gratefully acknowledge support of this work by the Swedish Wennergren foundation, the Knut and Alice Wallenberg Foundation, the Swedish Foundation for International Cooperation in Research and Higher education (STINT), the Göran Gustavssons Stiftelse, the Swedish Natural Research Council (NFR), the Swedish Foundation for Strategic Research (SSF) through a Senior Individual Grant, and the Swedish Research Council for Engineering Sciences (TFR).

-
- [1] F. Gel'mukhanov and H. Ågren, *Phys. Rep.* **312**, 87 (1999).
[2] G.B. Armen, H. Aksela, T. Åberg, and S. Aksela, *J. Phys. B* **33**, R49 (2000).
[3] For recent references see, e.g., N. Mårtensson, O. Karis, and A. Nilsson, *J. Electron Spectrosc. Relat. Phenom.* **100**, 379 (2000), and other articles in that volume.
[4] A.J. Yencha *et al.*, *Chem. Phys.* **238**, 109 (1998).
[5] P. Natalis, P. Pennetreau, L. Longton, and J.E. Collin, *Chem. Phys.* **73**, 191 (1982).
[6] M. Bässler *et al.*, *J. Electron Spectrosc. Relat. Phenom.* **101-103**, 953 (1999).
[7] D. Edvardsson *et al.*, *J. Electron Spectrosc. Relat. Phenom.* **73**, 105 (1995).
[8] R. Feifel *et al.*, *Phys. Rev. Lett.* **85**, 3133 (2000).
[9] P. Salek, F. Gel'mukhanov, and H. Ågren, *Phys. Rev. A* **59**, 1147 (1999).
[10] E. Kukk *et al.*, *Phys. Rev. A* **57**, R1485 (1998).
[11] O. Björneholm *et al.*, *Phys. Rev. Lett.* **79**, 3150 (1997).
[12] E. Kukk *et al.*, *Phys. Rev. Lett.* **76**, 3100 (1996).
[13] Z.F. Liu, G.M. Bancroft, J.S. Tse, and Z.Z. Yang, *Chem. Phys.* **192**, 255 (1995).
[14] H. Aksela *et al.*, *Phys. Rev. A* **45**, 7948 (1992).
[15] R.F. Fink, M. Kivilompolo, and H. Aksela, *J. Chem. Phys.* **111**, 10 034 (1999).
[16] R.F. Fink, M. Kivilompolo, H. Aksela, and S. Aksela, *Phys. Rev. A* **58**, 1988 (1998).
[17] M. Kivilompolo *et al.*, *J. Phys. B* **33**, L157 (2000).
[18] K. Ellingsen, T. Saue, H. Aksela, and O. Gropen, *Phys. Rev. A* **55**, 2743 (1997).
[19] H. Aksela *et al.*, *J. Phys. B* **28**, 4259 (1995).
[20] G. Herzberg, *Molecular Spectra and Molecular Structure* (Van Nostrand Reinhold, New York, 1955), Vol. 2.
[21] H. Pulkkinen *et al.*, *J. Phys. B* **29**, 3033 (1996).
[22] S. Svensson *et al.*, *Phys. Rev. Lett.* **72**, 3021 (1994).
[23] F. Gel'mukhanov *et al.*, *Phys. Rev. A* **53**, 1379 (1996).